A Robotic System with Robust Remote Center Motion Constraint for Endometrial Regeneration Surgery

Jianhua Li
Shenyang Institute of Automation Chinese Academy of Sciences
Chongyang Wang
Shenyang Institute of Automation Chinese Academy of Sciences
Zhenxing Wang
Shenyang Institute of Automation Chinese Academy of Sciences
Xiong Zheng
Shenyang Jianzhu University
Zhidong Wang
Chiba Institute of Technology: Chiba Kogyo Daigaku
Jichun Tan
China Medical University
Hao Liu (liuhao@sia.cn)
Shenyang Institute of Automation Chinese Academy of Sciences

Original Article

Keywords: Endometrial Regeneration, Surgical Robot, Remote

Posted Date: August 30th, 2021

DOI: https://doi.org/10.21203/rs.3.rs-845703/v1

Title page

A Robotic System with Robust Remote Center Motion Constraint for Endometrial Regeneration Surgery

Jian-Hua Li, born in 1992, is currently a PhD candidate at *State Key Laboratory of Robotics, Shenyang Institute of Automation, Chinese Academy of Sciences, and University of Chinese Academy of Science, China*. He received his bachelor degree from *Central South University, China*, in 2016. His research interests include medical robots and systems, continuum robots, and robot control.
Tel: +86-024- 83602925; E-mail: lijianhua@sia.com

Chong-Yang Wang, born in 1991, is currently a research assistant at *Shenyang Institute of Automation, Chinese Academy of Sciences, China*. He received the B.E. and M.E. degrees from *Harbin Institute of Technology, China*, in 2013 and 2015, respectively. His research interests include surgical robots, medical sensors and robot control.
Tel: +86-024- 83602925; E-mail: wangchongyang@sia.cn.

Zhen-Xing Wang, born in 1995, is currently a PhD candidate at *State Key Laboratory of Robotics, Shenyang Institute of Automation, Chinese Academy of Sciences, and University of Chinese Academy of Science, China*. He received his bachelor degree from *Taiyuan University of Technology, China*, in 2018. His research interests include design and control of surgical robotics, continuum robots, and human–robot interaction.
E-mail: wangzhenxing@sia.com

Xiong Zheng, born in 1996, is currently a master degree candidate of *Mechanical Engineering College of Shenyang Jianzhu University, China*. He received his bachelor degree from *Anhui Jianzhu University, China*, in 2019. His research interests include medical robots and systems, vascular interventional surgery robots and robot control.
E-mail: zhengxiong312@163.com

Zhi-Dong Wang, is currently a Professor at the Department of Advance Robotics, Chiba Institute of Technology, Japan. He received the B.S. degree from the Beijing University of Aeronautics and Astronautics, Beijing, China, in 1987. He received the M.S. and Ph.D. degrees from the Graduate School of Engineering, Tohoku University, Sendai, Japan, in 1992 and 1995, respectively. His current research interests include human-robot interaction and cooperation systems, distributed autonomous robot systems, micro/nano robotics, and application of intelligent robot technologies for the disabled
E-mail: Zhidong.wang@it-chiba.ac.jp

Ji-Chun Tan, born in 1965, is a professor at Shengjing Hospital Affiliated to China Medical University, China. She received the B.S., M.S. and Ph.D. degrees from Jilin University, China, in 1986, 1989 and 2003, respectively. Her research interests include infertility, assisted reproductive technology, stem cells, and surgical robot.
E-mail: tjczjh@163.com

Hao Liu, born in 1980, is currently a professor at *Shenyang Institute of Automation, Chinese Academy of Sciences, China*. He received the B.S., M.S., and Ph.D. degrees in mechanical engineering from the *Harbin Institute of Technology, China*, in 2004, 2006, and 2010, respectively. He worked as a visiting scholar in *Laboratory for Computational Sensing and Robotics, Johns Hopkins University, United States of America* from 2014-2015. His research interests include surgical robots, medical sensors, surgical navigation, and robot control.
Tel: +86-024- 83602067; E-mail: liuhao@sia.cn

Corresponding author：Hao Liu　E-mail：liuhao@sia.com

ORIGINAL ARTICLE

A Robotic System with Robust Remote Center of Motion Constraint for Endometrial Regeneration Surgery

Jian-Hua Li[1, 2,3] • Chong-Yang Wang[1,2] • Zhen-Xing Wang[1,2,3] • Xiong Zheng[4] • Zhi-Dong Wang[5] • Ji-Chun Tan[6] • Hao Liu[1,2]

Received June xx, 201x; revised February xx, 201x; accepted March xx, 201x

Abstract: Surgical robots have been widely used in various surgeries in order to improve and facilitate the surgeries. However, there is no robot intended for endometrial regeneration surgery which is a new therapy to restore women's fertility by using stem cells. Endometrial regeneration surgery requires processing endometrium and transplanting stem cells with the minimal trauma to uterus. In this paper, we introduce a surgical robotic system which consists of a dexterous hysteroscope, a supporting arm and additional novel instruments to facilitate the operations and decrease trauma to the uterus. To protect the cervix of the uterus, remote center of motion (RCM) constraint is required. First, the supporting arm and the hysteroscope are controlled separately in kinematics in order to ensure that the RCM constraint and the hysteroscope's shape and posture are predictable. Then, a task decoupled method is used to improve the robustness of the RCM constraint. The experiments show that our method is more robust and achieves higher accuracy of RCM. Besides, the master slave control of robot with RCM constraint is also verified.

Keywords: Endometrial Regeneration • Surgical Robot • Remote Center of Motion • Task Decoupled

✉ Hao Liu
liuhao@sia.cn

1 State Key Laboratory of Robotics, Shenyang Institute of Automation, Chinese Academy of Sciences, Shenyang 110016, China

2 Institutes for Robotics and Intelligent Manufacturing, Chinese Academy of Sciences, Shenyang 110169, China

3 University of Chinese Academy of Sciences, Beijing 100049, China

4 Shenyang Jianzhu University, Shenyang, 110168, China

5 Chiba Institute of Technology, Chiba, 275-0016, Japan

6 Shengjing Hospital affiliated to China Medical University, Shenyang, 110016, China

1 Introduction

According to the data from world health organization, the increasing number of infertile females has been 30 million in the world[1]. Intrauterine adhesions (IUAs) are a major cause of secondary infertility and most of IUAs are associated with damage to the uteri due to intrauterine surgery[2]. Traditional remedies like transcervical resection of adhesions and artificial hormone therapy bear high recurrence rate of IUAs. Recently, stem cell therapy is a promising remedy to fundamentally cure endometrial damage[3-5]. Creating transplant wound and transplanting stem cells are two key steps for endometrial regeneration surgery, as shown in Figure 1. However, the handheld instruments and manual operation methods make the surgery difficult and confine the efficacy of this new therapy. What's more, these operations may cause secondary damage to the uterus. During endometrial regeneration surgery, a hysteroscope is inserted into the uterine cavity via cervix. The motion of the hysteroscope is constrained by the cervix, which can be considered as remote center of motion constraint. To facilitate the process and improve the outcome of stem cell therapy, a robot intended for endometrial regeneration surgery is required.

Many robotics has been designed by researchers for diverse surgeries[6-9]. Da Vinci surgical system is the most successful commercial surgical robot. Though it has be used to perform hysterectomy, a surgery to remove patient's uterus, it has no ability to process the endometrium without hurting the uterus[10]. Another surgical robot, Hominis surgical system, is designed for single site, transvaginal surgical procedures[11]. It is also not applicable for endometrial regeneration surgery since its instruments work outside the uterus. Besides, there are many robotic systems intended for natural orifice transluminal endoscopic surgeries. He et. al. proposed a robot-assisted method to perform nasal surgery[12]. Amanov et. al. design a surgical system by using concentric tube robots to finish prostatectomy in the small luminal space of the urethra[13]. Similarly, Goldman et al. present a continuum robot for transurethral surgeries[14]. Andrea et al. introduce an endonasal telerobotic system which is used in the micro-surgery of the throat[15]. Shang et. al. design a single-port robotic system for transcanal microsurgery[16]. Lau et al. design a flexible surgical robotic system for endoscopic submucosal dissection[17]. These robots achieved great progress in kinds of natural orifice transluminal surgeries.

During endometrial regeneration surgery, the motion of the hysteroscope suffers from the RCM constraint. The RCM constraint is a popular problem for laparoscopic surgery and ophthalmic microsurgery[7, 18]. Mechanical RCM and programmable RCM are two main ways to realize RCM constraint during surgical manipulation. In the context of mechanical RCM, many researchers propose mechanical structures to realize RCM constraints. He et al. designed a novel remote center of motion mechanism for the robot of retinal vascular bypass surgery[19]. Kim et al. propose a novel gravity compensation mechanism with RCM mechanisms[20]. Different with mechanical RCM, programmable RCM is realized by the software and is more flexible. To realize RCM constraint, two DOFs of the robot are required. Aghakhani et al. provide a general method to realize the surgical robot's control task with RCM constraint by using the kinematics of extended task[21]. Similarly, Sadeghian et al. combine the task with the RCM constraint into a RCM-constraint Jacobian[22]. However, the extended task Jacobian is easy to be singularity. Tangent plane of the access port is also used to express the kinematics of the RCM point[23]. However, determining the tangent plane is difficult during applications. Sandoval et al. associate the RCM constraint with the task space by using the minimum distance between surgical tool with the RCM point[24]. Using the null space of the robot provides another way to realize the RCM constraint[25-27]. To guarantee the RCM, redundant robot is required. Besides, Zhang and Li et al. realize the endoscope's visual tracking control with RCM constraints[27, 28].

Examining the existing surgical robots, many of them facilitate and improve kinds of surgeries while none of them is intended for endometrial regeneration surgery. In our previous works, a continuum manipulator is designed to reach the targets on the endometrium[29]. For endometrial regeneration surgery, the robot is required to perform multiple tasks in the confined uterine cavity while ensuring the safety of the uterus. In order to protect the cervix of the uterus, the hysteroscope should be manipulated with the RCM constraint. In this paper, we design a robotic system to facilitate the operations and protect the uterus during the endometrial regeneration surgery. To maintain the flexibility while improve the stability of the robot, we propose a task decoupled method to control the hysteroscope with robust RCM constraint. The method is evaluated by comparing with the general method, extended task method. The control method of the robot is also verified in experiments.

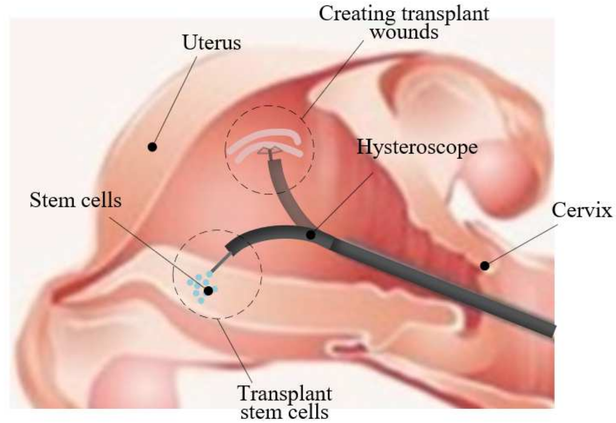

Figure 1 The operations during endometrial regeneration surgery.

This paper is organized as follows: Section 2 introduces the surgical procedure and the design of the robotic system. Section 3 details the kinematics of the robot, the realization of the RCM constraint and the control method of the robot. Section 4 presents the experiments and the results. Section 5 is the conclusion.

2 Design of the Robotic System

2.1 Surgical Procedure and Requirements

In endometrial regeneration surgery, the ultimate goal is to transplant stem cells into the uterus and realize the regeneration of the endometrium. To successfully perform endometrial regeneration surgery, tasks like diagnosing uterine cavity and processing endometrium are required before transplanting stem cells. The procedure of endometrial regeneration surgery is list as following:

(1) Insert the hysteroscope into the vagina, though cervix and into the uterus.

(2) Observe the uterine cavity, find the uterine horn, and

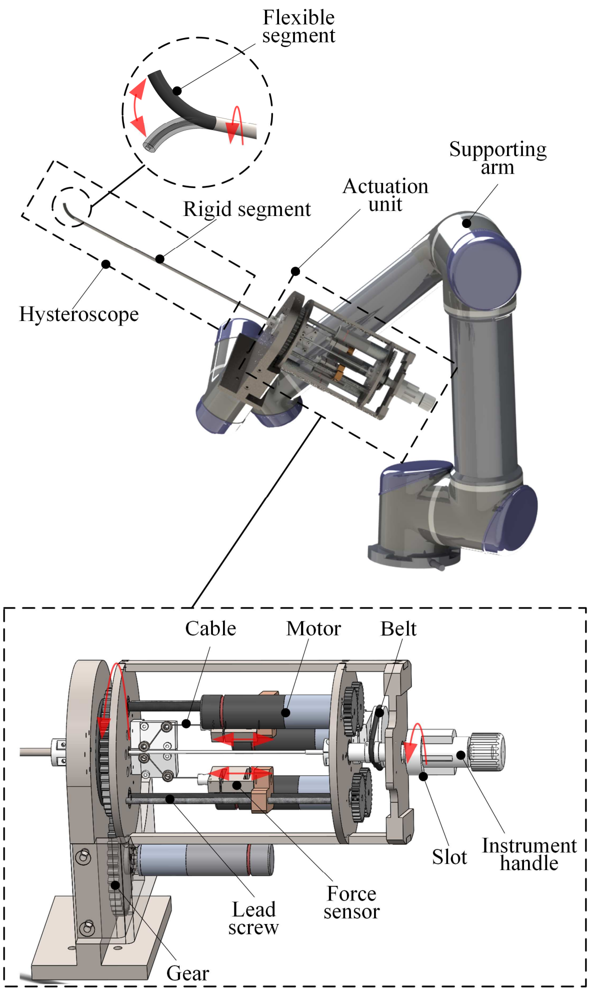

Figure 2 Structure details of the flexible hysteroscope and the actuation unit.

determine the position of transplantation.

(3) Insert the instrument of making wound through the channel of the hysteroscope into the uterine cavity. Control the hysteroscope to locate the tip of the instrument to the position of adhesions. Scratch the endometrium to remove the adhesions and create regeneration environment for stem cells.

(4) Replace the instrument of making wound to transplant instrument. Transplant the stem cells on the transplant wounds.

According to the procedure of endometrial regeneration surgery, the hysteroscope is required to have small size and high dexterity in order to perform operation in the uterine cavity. The small size of the hysteroscope can decrease the invasion to the cervix. The high dexterity enables the hysteroscope to avoid pulling to the cervix during operation in uterine cavity. The instruments should be small enough to pass through the channel of the hysteroscope. The instrument of making wound should be capable to scratch the endometrium with high quality and high efficiency.

2.2 Design of the Dexterous Hysteroscope

Hysteroscope is the key part for the surgical system. It feedbacks the view of uterine cavity and provides channels for other instruments. The traditional rigid hysteroscopes are hard and have low dexterity, which may cause damage to the endometrium and the cervix. Some flexible diagnostic hysteroscopes have the advantages of smaller size and high compliance to ensure safety during diagnostics. However, these devices are not feasible to manipulate and suffer from poor load capability. To overcome these difficulties, we design a hysteroscope which has a flexible tip and a rigid shaft body, as shown in Figure 2. The hysteroscope provide an inner channel for the instruments which are used to process endometrium or transplant stem cells. The diameter of the hysteroscope is 5 mm and the diameter of the inner channel is 2.5 mm. The length of the flexible segment is 30 mm. The flexible segment of the hysteroscope is driven by two cables and can realize planar deformation. The rigid segment of the hysteroscope is fixed on the actuation unit. The actuation unit has two lead screws which are used to pull the cables. To acquire the pulling force, the two cables are separately fixed on two force sensors and the sensors are installed on the lead screws. Besides, a pair of gears is used to realize the hysteroscope's rotation along the axis of the rigid segment. In the end of the actuation unit, there is a slot where the additional instrument can be inserted. By actuating the slot, the instrument can rotate along its axis. To increase the dexterity of the hysteroscope, a supporting arm is used to provide additional DOFs for the hysteroscope to realize motions with RCM constraint.

2.3 Design of the Additional Instruments

Two kinds of instruments are used in endometrial regeneration surgery. One is the instrument for scratching

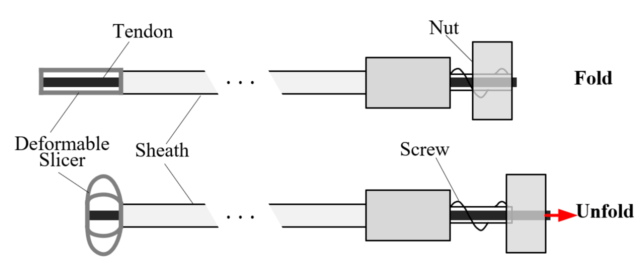

Figure 3 The design of the instrument for scratching the endometrium. The slicer can be unfolded by screwing the nut and pulling the tendon.

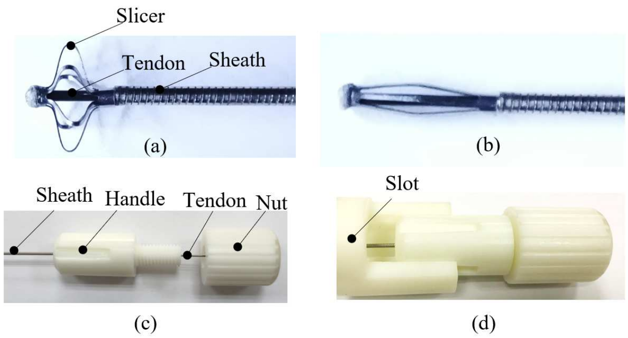

Figure 4 Instrument for scratching the endometrium. (a) the condition of the unfolded slicer. (b) the condition of the folded slicer. (c) the structure of the instrument at the proximal end. (d) the instrument is inserted in the slot of the actuation unit.

the endometrium. It is composed of a lantern-like slicer, a sheath tube and a handle. The slicer has multiple thin beams which can be deformed easily. One end of the slicer is supported by the sheath tube. The other end of the slicer is fixed with the tip of a tendon which passes through the slicer and the sheath. When pulling the tendon, the slicer can be unfolded. The handle is used to control the slicer to fold or unfold. The handle is composed of two parts that one part is fixed with the sheath and the other part, liking a nut, is fixed with the other tip of the tendon. By screwing the nut, the tendon is pulled or pushed resulting that the slicer is unfolded and folded. When the slicer is folded and unfolded, their maximal diameters are 1.5 mm and 6mm separately. When the slicer is folded, it can pass through the channel in the hysteroscope. Then, the handle is inserted into the slot of the actuation unit. When the slicer reaches the uterine cavity, the slicer can be unfolded by screwing the nut. Then, the deformed beam of the slicer contacts

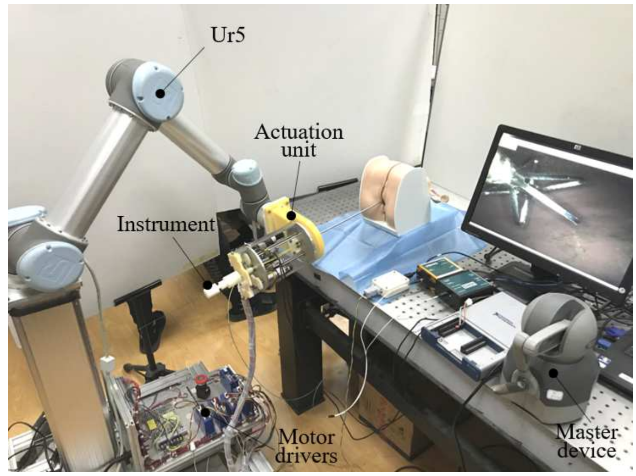

Figure 5 The overview of the robotic system. The monitor shows the view that the unfolded slicer.

with the tissues of the endometrium. When actuating the slot, the slicer is rotated to scratch the endometrium. The slicer is made of thin-wall nitinol tube with outer diameter (OD) = 1.27 mm and inner diameter (ID) = 1.07 mm. The thin beams are manufactured by grooving the tube with the method of laser cutting. The width of the groove is 0.35 mm and the length of the groove is 6.5 mm. The number of the groove is 6. The other instrument is a long tube which is used to transmit stem cell suspension. The tube can also pass through the channel of the hysteroscope. The tube is connected with a syringe which is used to control the injection volume of stem cell suspension.

2.4 Integration of the Robotic System

The robotic system for endometrial regeneration surgery is

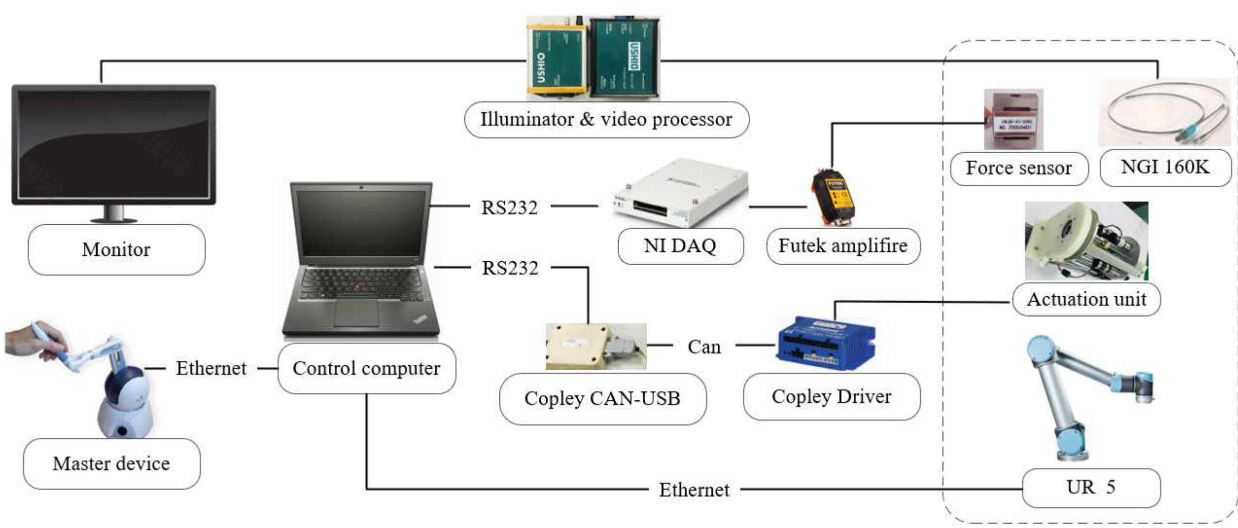

Figure 6 System architecture of the robotic system.

shown in Figure 5. It consists of a supporting arm, an actuation unit, a dexterous hysteroscope, and a master device. The surgeon can view the uterine cavity on a monitor and control the motion of the hysteroscope by manipulating the master device. The UR5 arm is used to support the actuation unit and provide additional DOFs to control the motion of the hysteroscope with the remote center of motion constraint. A camera with a resolution of 400×400 pixels is fixed in the hysteroscope to view the uterine cavity. The diameter of the camera is 1.7 mm. There are four motors at the actuation unit. Two of them are used to actuate lead screws to pull the cables. One of them is used to actuated the gears to rotate the hysteroscope. The last one is used to actuate the belt pulley to rotate the slicer. All motors are powered by drivers (Copley Driver; USA) and controlled by a controller (Copley CAN-USB; USA). Besides, two force sensors are used to feedback the actuation force. The sensors are connected with two amplifiers (Futek; USA). A data acquisition equipment (NI DAQ; USA) is used to acquire the force data. Figure 6 shows the architecture of the robotic system.

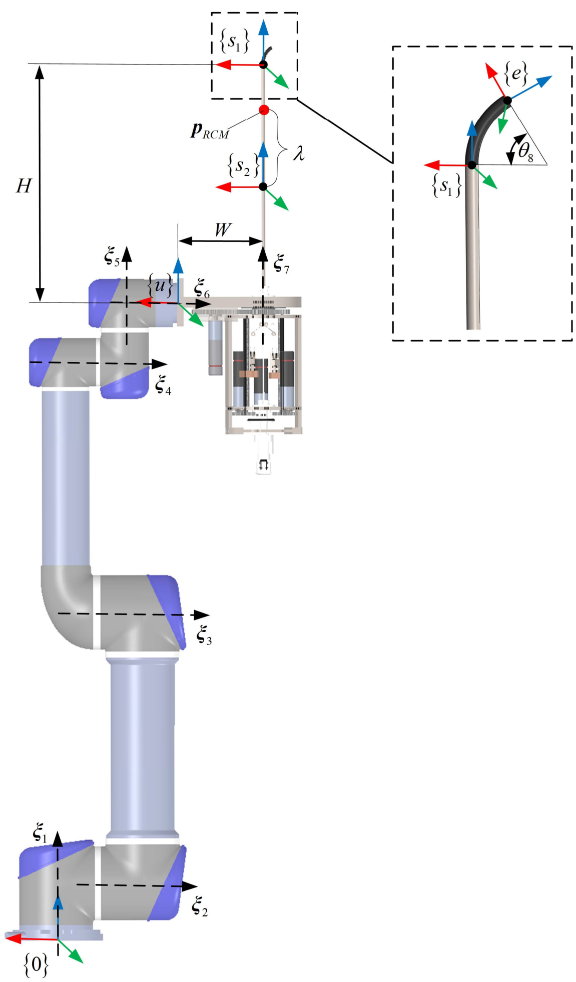

Figure 7 Constraint of remote center of motion and coordinate frames.

3 Methodology

In this section, we introduce the direct kinematics of the surgical robot and the realization of the RCM constraint. Finally, the control method of the whole surgical robot is introduced.

3.1 Kinematics of the Surgical Robot

For the surgical system, the motion of the hysteroscope's distal tip is related with the actuation unit and the supporting arm. The actuation unit provide two DOFs including rotation of the rigid segment and the bending of the flexible segment. The UR5 arm supports the hysteroscope unit and provides the DOFs for remote center motion and controls the position of the rigid segment of the hysteroscope. We define the joint vector of the UR5 arm as $\boldsymbol{q}_u=[\theta_1,\theta_2,\ldots\theta_6]^T$. The forward kinematics of the UR5 arm is expressed as

$$ {}^{0}\boldsymbol{T}_u(\boldsymbol{q}_u)=\prod_{i=1}^{6} e^{\hat{\xi}_i\theta_i}\cdot{}^{0}\boldsymbol{M}_u \tag{1}$$,

where ξ_i is the screw axis of the i^{th} joint and ${}^{0}\boldsymbol{M}_u$ is the transformation matrix from frame $\{u\}$ to frame $\{0\}$ when the joint values are zeros, as shown in Figure 7. For the actuation unit, the rotation angle of the rigid segment and the bending angle of the flexible segment are separately defined as θ_7 and θ_8. Then, the transformation matrix of the tip of the hysteroscope is expressed as

$$ {}^{0}\boldsymbol{T}_e={}^{0}\boldsymbol{T}_u\cdot e^{\hat{\xi}_7\theta_7}\cdot{}^{u}\boldsymbol{M}_{s1}\cdot e^{\hat{\xi}_8 L} \tag{2}$$,

where ξ_7 and ξ_8 are separately the screw axis of the two additional joints, $\{s_1\}$ is the frame related with tip of the rigid segment, ${}^{u}\boldsymbol{M}_{s1}$ is the transformation matrix from frame $\{s_1\}$ to frame $\{0\}$ when $\theta_7=0$, and L is the length of the flexible segment. ξ_7 has the format of

$$\xi_7=[0,W,0,0,0,1]^T \tag{3}$$,

and ξ_8 has the format of

$$\xi_8=\left[0,0,1,0,\frac{\theta_8}{L},0\right]^T \tag{4}$$.

${}^{u}\boldsymbol{M}_{s1}$ has the format of

$$ {}^{u}\boldsymbol{M}_{s1}=\begin{bmatrix}1&0&0&-W\\0&1&0&0\\0&0&1&H\\0&0&0&1\end{bmatrix} \tag{5}$$,

where H and W are separately the distance between frame $\{s_1\}$ and frame $\{u\}$ in x-axis direction and z-axis direction, as shown in Figure 7. Finally, the direct kinematics of the robot is expressed.

3.2 Remote Center of Motion Constraint

During endometrial regeneration surgery, the hysteroscope should passe through cervix to reach the uterine cavity. The motion of the rigid segment is constrained by the cervix, which is considered as RCM constraint. To express the point on the rigid segment which instantaneously coincident with the position of the cervix, a variable related with the insertion depth is used [21]. As shown in Figure 7, the RCM point on the rigid segment is expressed as

$$\begin{aligned} &\boldsymbol{p}_{RCM} = \boldsymbol{p}_{s2} + \lambda(\boldsymbol{p}_{s1} - \boldsymbol{p}_{s2}) \\ &0 \le \lambda \le 1 \end{aligned} \tag{6},$$

where $\boldsymbol{p}_{s1}$ express the position of the rigid segment's distal tip, $\boldsymbol{p}_{s2}$ is the position of another fixed point on the rigid segment, and λ is the parameter which implies the insertion degree. For the two fixed points on the rigid segment, their Jacobians are expressed as

$$\begin{aligned} \boldsymbol{J}_{s1} &= Ad_{T_1}\left(\boldsymbol{J}_u^s\right) \\ \boldsymbol{J}_{s2} &= Ad_{T_2}\left(\boldsymbol{J}_u^s\right) \end{aligned} \tag{7},$$

where $\boldsymbol{J}_u^s$ is the spatial Jacobian of the UR5 arm, $\boldsymbol{T}_1$ and $\boldsymbol{T}_2$ are two homogeneous matrixes which are separately related with $\boldsymbol{p}_{s1}$ and $\boldsymbol{p}_{s2}$. The two homogeneous matrixes have the format of

$$\begin{aligned} \boldsymbol{T}_1 &= \begin{bmatrix} \boldsymbol{I}_{3\times3} & \boldsymbol{p}_{s1} \\ 0 & 1 \end{bmatrix} \\ \boldsymbol{T}_2 &= \begin{bmatrix} \boldsymbol{I}_{3\times3} & \boldsymbol{p}_{s2} \\ 0 & 1 \end{bmatrix} \end{aligned} \tag{8}.$$

According to (6), the differential format of the RCM point is derived as

$$\dot{\boldsymbol{p}}_{RCM} = \begin{bmatrix} \boldsymbol{J}_{s1,v} + \lambda\left(\boldsymbol{J}_{s2,v} - \boldsymbol{J}_{s1,v}\right) \\ \boldsymbol{p}_{s2} - \boldsymbol{p}_{s1} \end{bmatrix}^T \begin{pmatrix} \dot{\boldsymbol{q}}_u \\ \dot{\lambda} \end{pmatrix} \tag{9},$$

where $\boldsymbol{J}_{s1,v}$ and $\boldsymbol{J}_{s2,v}$ are separately the translational part of the of $\boldsymbol{J}_{s1}$ and $\boldsymbol{J}_{s2}$.

For the supporting arm, two tasks are required including tracking the desired position of the rigid segment tip and ensuring the RCM point coincide with the position of cervix. First, we define the error of RCM as

$$\boldsymbol{e}_{RCM} = \boldsymbol{p}_c - \boldsymbol{p}_{RCM} \tag{10},$$

where $\boldsymbol{p}_c$ is the desired position of remote center, *i. e.*, the position of the cervix. Different with the work of [22] which combines the two tasks into an extended task, we propose a task decoupled method to realize robust RCM constraint. In our method, RCM constraint is considered as the primary task and position tracking is achieved by using the null space projector of the Jacobian of RCM. This method does not increase the dimension of the algorithm Jacobian so that algorithm singularity can be avoided. Besides, the error of the RCM can be maintained at a low level since RCM constraint is the primary task in the algorithm. However, position tracking may fail if the instantaneous motion of position tracking conflict with RCM constraint. To ensure the task of position tracking not to conflict with the RCM constraint task, the instantaneous motion of position tracking is decoupled into insertion motion and directional motion, as shown in Figure 8. For the RCM constraint, whether the insertion motion or the rotation motion will not cause error of the RCM. Finally, the joint velocity of the supporting arm is expressed as

$$\dot{\boldsymbol{q}}_u = \boldsymbol{J}_{RCM}^{\#}\boldsymbol{e}_{RCM} + \left(\boldsymbol{I} - \boldsymbol{J}_{RCM}^{\#} \cdot \boldsymbol{J}_{RCM}\right)\left[\dot{\boldsymbol{q}}_r \quad \dot{\lambda}\right]^T \tag{11}.$$

where $\boldsymbol{J}_{RCM}^{\#} = \boldsymbol{J}_{RCM}{}^T\left(\boldsymbol{J}_{RCM} \cdot \boldsymbol{J}_{RCM}{}^T\right)^{-1}$ is the pseudoinverse of the RCM Jacobian, $\dot{\boldsymbol{q}}_r$ is related with the directional motion and $\dot{\lambda}$ is related with the insertion motion. To get the value of $\dot{\boldsymbol{q}}_r$ which is used to realize the directional motion, we should define the direction error. For the rigid segment, its desired direction $\boldsymbol{r}_{s1,z}$ can be easily got by using the desired position and the position of cervix. The desired direction of the rigid segment is written as

$$\boldsymbol{r}_{s1,z} = \left(\boldsymbol{p}_{s1,d} - \boldsymbol{p}_c\right) / \left|\boldsymbol{p}_{s1,d} - \boldsymbol{p}_c\right| \tag{12},$$

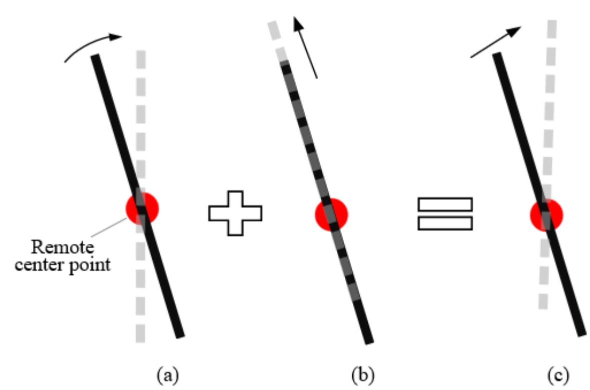

Figure 8 The motion of hysteroscope with RCM constraint. (a) Pure directional motion. (b) Pure insertion motion. (c) The hybrid motion of directional motion and insertion motion.

where $\boldsymbol{p}_{s1,d}$ is the desired position of the tip of the rigid segment. Then, the direction error of the rigid segment is expressed as

$$f_e(\boldsymbol{q}_u)=\boldsymbol{r}_{s1,z}^T\cdot(\boldsymbol{p}_{s1}-\boldsymbol{p}_{s2})/|\boldsymbol{p}_{s1}-\boldsymbol{p}_{s2}| \qquad (13).$$

By using the gradient of the direction error, $\dot{\boldsymbol{q}}_r$ is got as

$$\dot{\boldsymbol{q}}_r=k_e\cdot\nabla\boldsymbol{f}_e/|\nabla\boldsymbol{f}_e| \qquad (14),$$

where k_e is a positive coefficient and $\nabla\boldsymbol{f}_e$ is the gradient of the direction error. For the insertion motion, $\dot{\lambda}$ is written as

$$\dot{\lambda}=k_\lambda(\lambda_d-\lambda) \qquad (15),$$

where k_λ is a positive coefficient and λ_d is the desired value of the insertion distance. By using (11), we can realize the reliable control of the position tracking of the rigid segment with remote center motion constraint.

3.3 Control of the Robot System

During the surgical process, not only the supporting arm but also the flexible segment of the hysteroscope should be controlled in order to reach the desired position with desired direction. Though the control of the whole robot system can be realized by using the inverse differential kinematics of the robot system, the bending angle of the flexible segment is unpredictable during the iterative process. We directly calculate the bending angle and the rotation angle of the flexible segment by using the inverse kinematics of the flexible segment. This ensures that the bending of the flexible segment is predicted. Therefore, the flexible segment and the supporting arm are controlled separately in kinematics, as shown in Figure 9. First, we identify the desired position of the RCM point in the robotic frame. After engaging the teach mode of the supporting arm, we can move the tip of the hysteroscope to the desired position. Using the feedback values of joints and the initial value of λ, we can get the initial value of $\boldsymbol{p}_{RCM}$ and the initial direction of the rigid segment $[\boldsymbol{r}_{init,x}\ \boldsymbol{r}_{init,y}\ \boldsymbol{r}_{init,z}]$. The relationship between the bending angle of the flexible segment θ_8 and the targets is shown in Figure 8. We use a parameter α to imply whether bending is required for the flexible segment to reach the desired direction. It is defined as

$$\alpha=\arccos\left(\boldsymbol{r}_d{}^T\cdot\frac{(\boldsymbol{p}_d-\boldsymbol{p}_{RCM})}{|\boldsymbol{p}_d-\boldsymbol{p}_{RCM}|}\right) \qquad (16),$$

where $\boldsymbol{p}_d$ is the desired position, $\boldsymbol{r}_d$ is the desired direction. When $\alpha=0$, it means no bending is required

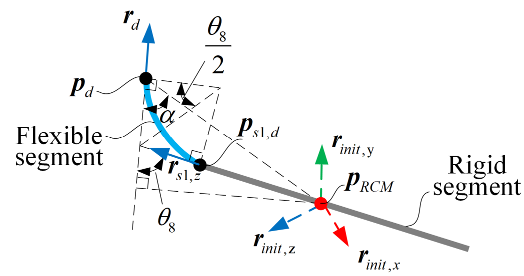

Figure 9 The geometric of the hysteroscope with RCM constraint when it reach the desired position with the desired direction.

for the flexible segment. In this condition, we have

$$\begin{aligned}\theta_7&=0\\ \theta_8&=0\\ \boldsymbol{r}_{s1,z}&=\boldsymbol{r}_d\\ \boldsymbol{p}_{s1}&=\boldsymbol{p}_d-L\cdot\boldsymbol{r}_d\end{aligned} \qquad (17).$$

We consider the condition of $\alpha\neq0$. According to Figure 9, we can get θ_8 by solving

$$\left(|\boldsymbol{p}_d-\boldsymbol{p}_{RCM}|\cos\alpha-\frac{|\boldsymbol{p}_d-\boldsymbol{p}_{RCM}|\sin\alpha}{\tan\theta_8}\right)\frac{\theta_8}{\tan(\theta_8/2)}=L \qquad (18),$$

where L is the length of the flexible segment. Next, we can get the desired direction of the rigid segment by using

$$\boldsymbol{r}_{s1,z}=\frac{\boldsymbol{p}_d-\frac{L}{\theta_8}\tan\left(\frac{\theta_8}{2}\right)\boldsymbol{r}_d-\boldsymbol{p}_{RCM}}{\left|\boldsymbol{p}_d-\frac{L}{\theta_8}\tan\left(\frac{\theta_8}{2}\right)\boldsymbol{r}_d-\boldsymbol{p}_{RCM}\right|} \qquad (19).$$

The desired position of the rigid segment tip is expressed as

$$\boldsymbol{p}_{s1,d}=\boldsymbol{p}_d-\frac{L}{\theta_8}\tan\left(\frac{\theta_8}{2}\right)\boldsymbol{r}_d-\frac{L}{\theta_8}\tan\left(\frac{\theta_8}{2}\right)\boldsymbol{r}_{s1,z} \qquad (20).$$

Besides, the rotation of the segment is also required to make the bending plane of the flexible segment parallels with the desired direction. The rotation angle θ_7 can be got by using

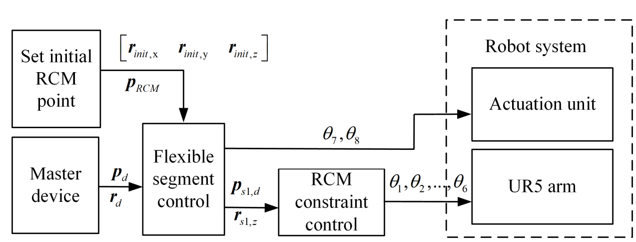

Figure 10 The diagram of the control method.

$$\theta_7 = \arccos\left(\left(\boldsymbol{r}_d \times \frac{(\boldsymbol{p}_d - \boldsymbol{p}_{RCM})}{|\boldsymbol{p}_d - \boldsymbol{p}_{RCM}|}\right)^T \cdot \hat{\boldsymbol{\omega}}_{s1} \cdot \boldsymbol{r}_{init,y}\right) \quad (21),$$

where $\hat{\boldsymbol{\omega}}_{s1}$ is the skew-symmetric of the rotation vector for the direction of rigid segment from $\boldsymbol{r}_{init,z}$ to $\boldsymbol{r}_{s1,z}$. It has the format of

$$\boldsymbol{\omega}_{s1} = \boldsymbol{r}_{init,z} \times \boldsymbol{r}_{s1,z} \quad (22).$$

Finally, the angles related with the flexible segment are all resolved. To control the supporting arm, $\boldsymbol{r}_{s1,z}$ and $\boldsymbol{p}_{s1,d}$ are used as the input of RCM control. The diagram of the control method for the robot system is shown in Figure 10.

4 Experiments

4.1 Parameters Identification of the Flexible Segment

To improve the control accuracy of the hysteroscope, the parameters including composite bending stiffness of the flexible segment and elastic coefficient of the cables should be identified. The hysteroscope's bending stiffness is different when different instruments in the channel. Therefore, we should consider three cases: no instrument is in the channel, the instrument of slicer is in the channel, the instrument of tube is in the channel. Figure 11 (a-c) shows the three cases. By pulling the cables, the flexible segment is separately deformed in different situations. The actuation force and the actuation displacement are record during the processes. In order to acquire the bend angle of the flexible segment, a colored label is attached on the tip of the flexible segment. The flexible segment is captured by a camera and its bending angle can be got by using the method in [30]. Figure 11 (d) shows the relations between the actuation force and the bend angle with different instruments in the hysteroscope. The bending stiffness of the three situations are separately 14.18 °/N, 5.77 °/N, and 8.06 °/N. When the instrument of slicer is in the channel, the flexible segment has biggest stiffness. Besides, we also get the elastic coefficient of the cables. The elastic coefficient is 0.076 mm/N.

4.2 RCM Constraint Evaluation in Simulation

In this section, we compare the task decoupled method (our method) with the general extended task method by simulation. All control algorithms are written in MATLAB. In the simulation, the robust and the accuracy of the two methods for RCM constraint are verified. First, the supporting arm is control to reach a target which has constant relative position of $[10, 0, 30]^T$ to the initial position. 200 random joint values with the range of $[-\pi, \pi]$ are used as the initial joint values. The initial

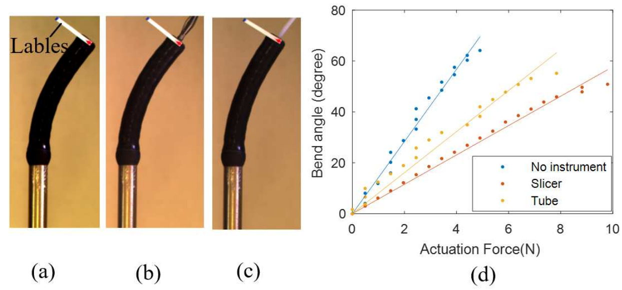

Figure 11 The flexible segment with different instruments in the channel. (a) No instrument is in the hysteroscope. (b) The instrument of slicer is in the hysteroscope. (c) The instrument of tube is in the hysteroscope. (d) The relationship between actuation force and bend angle.

value of λ is set as 0.8. During the process of reaching the desired position, algorithmic singularities or joint limits may be encountered. Therefore, not all the initial joint values led to successfully performing task. We record the times of successfully reaching the desired positions, the numbers of iterations, and the error of RCM when using the two control methods. The results are listed in Table 1. Task decoupled method is more robust for different initial gestures of the supporting arm. Though our method requires a larger number of iterations than extended task method, it achieves more accurate RCM constraint. Next, the supporting arm is controlled to reach different targets with the same initial joint values. The relative position of the target is set as $[x, y, 30]^T$. The range of x and y is

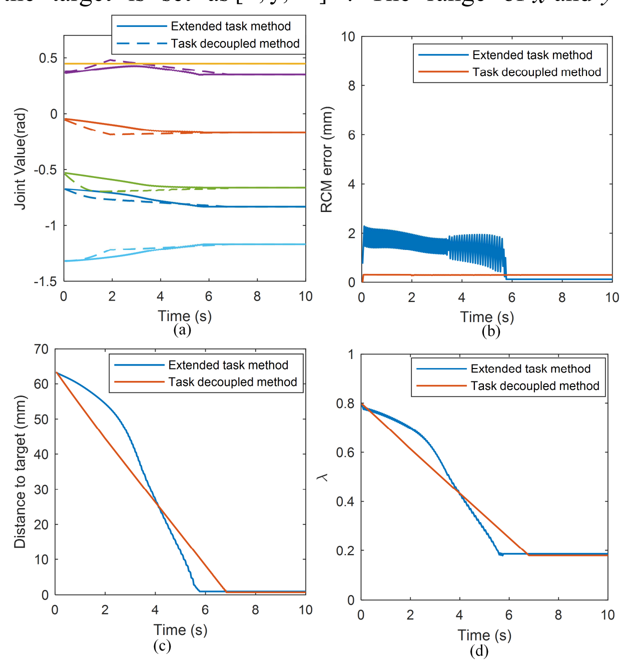

Figure 12 Simulation results for the robot to reach the target with RCM constraint by using two different methods, extended task method and tasks decoupled method (our method).

$[-30, 30]$. Similarly, 200 random values of x and y are used. In the simulation, four cases with different initial joint values are performed by separately using task decoupled method and extended task method. The results are listed in Table 2. According to Table 2, task decoupled method can cover most random targets and achieve higher success rates. Therefore, it is more robust for the supporting arm to reach different targets with different initial joint values. Furthermore, our method ensures low errors of RCM which are smaller than 0.6 mm. Besides, Figure 12 shows the variation of the parameters during reaching a target by using the two methods. For task decoupled method, the variation of λ is uniform and the RCM error is maintained in a stable low level. This is due in large part to the decoupling of tracking task and RCM constraint. The conflict of the two tasks is well avoided.

Table 1 Reach target with random initial joint values

Method	*Success rate*	*Mean number of iterations*	Mean e_{RCM}
Extended task	52/200	87	3.86
Task decoupled	141/200	153	0.68

Table 2 Reach random targets with the same initial joint values

Method		*Success rate*	*Mean number of iterations*	Mean e_{RCM}
Extended task	Case 1	103/200	112	2.04
	Case 2	64/200	189	4.16
	Case 3	0/200	-	-
	Case 4	0/200	-	-
Task decoupled	Case 1	122/200	290	0.56
	Case 2	182/200	216	0.30
	Case 3	154/200	265	0.34
	Case 4	135/200	173	0.42

4.3 Master Slave Control Evaluation

In this part, we experimentally evaluate the robot in master slave control mode. The core control algorithm of the robot which is written in MATLAB is integrated into a C++ shared library. Then, the library is called by a C++ program which is used to control all the devices including supporting arm, actuation unit, master device, etc. Besides, the motion of the robot is also visualizable at real time in a robotics simulation software (CoppeliaSim). To constraint the motion of the robot, the hysteroscope is inserted into a hole on an acrylic plate. The diameter of the holes is 5 mm and the hole is considered as the RCM point. The master device is manipulated by an operator. The tip of the robot is controlled to track the desired position and the desired direction commanded by the master device with the frequency of 50 Hz. The results of the experiment are illustrated in Figure 13. The results show that the rigid segment of the hysteroscope is well constrained by the RCM point during the whole manipulation process. Besides, the tip of the hysteroscope can reach different positions with different directions though the motion of the robot is constrained by the RCM point.

5 Conclusions

(1) In this paper, we introduce a robotic system with robust RCM constraint for endometrial regeneration surgery. The robotic system is intended to perform the two key processes of processing endometrium and transplanting stem cells during the surgery. To the best of the author's acknowledge, this is the first robot for the endometrial regeneration surgery.

(2) The robot is mainly composed of a dexterous hysteroscope, an actuation unit, and a supporting arm. It has high dexterity and compliance. To ensure the RCM constraint and make the hysteroscope's shape and posture predictable, the supporting arm and the hysteroscope are controlled separately in kinematics. Besides, a novel instrument which can be folded and unfolded is designed to process the endometrium.

(3) To improve the robustness and the flexibility of the RCM constraint, we propose a task decoupled method to ensure the RCM constraint. The RCM constraint is considered as the primary task and the tip position tracking is realized by using the null space of the RCM Jacobian. To avoid the confliction between RCM constraint and tip motion, the motion of the rigid

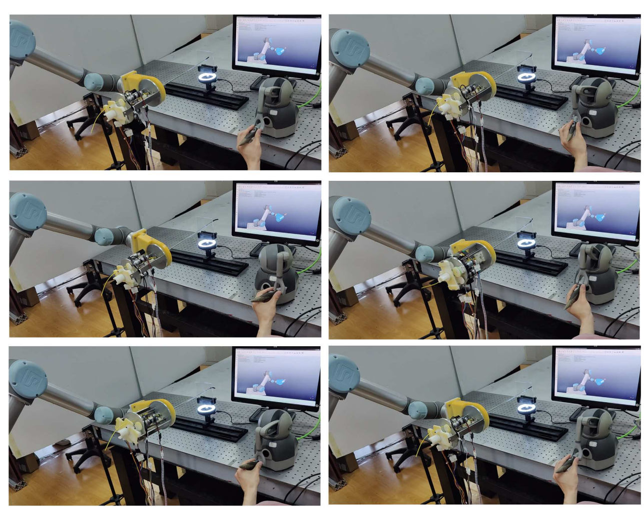

Figure 13 With RCM constraint, the robot is controlled to track desired position and desired direction in master slave control mode.

segment of the hysteroscope is decoupled into insertion motion and directional motion which are all orthogonal with the RCM constraint motion.

(4) The experiments show that the task decoupled method is more robust than the extended task method. The task decoupled method also achieves high RCM accuracy. Finally, the robot with RCM constraint is verified in master slave control.

6 Declaration

Acknowledgements

The authors sincerely thanks to Doctor Xing Xin of China Medical University for his advice in the design of the robot system.

Funding

Supported by National Natural Science Foundation of China (Grant No.61873257), Natural Science Foundation of Liaoning Province (2019-KF-01-12), Research Program of Shenzhen Institute of Artificial Intelligence and Robotics for Society (ACO1202005005), and Xingliao Talent Program (Grant No. XLYC1807078).

Availability of data and materials

The datasets supporting the conclusions of this article are included within the article.

Authors' contributions

The author' contributions are as follows: JL wrote the manuscript. CW, XZ, JT participated in the design of the robotic system. ZW, HL and ZW designed and assisted the experiments. All authors read and approved the final manuscript.

Competing interests

The authors declare no competing financial interests.

Consent for publication

Not applicable

Ethics approval and consent to participate

Not applicable

References

[1] W H Organization. Meeting to develop a global consensus on preconception care to reduce maternal and childhood mortality and morbidity. *World Health Organization Headquarters Geneva 6&ndash*;7 February 2012: Meeting report, 2013.

[2] S Warembourg, S Huberlant, X Garric, S Leprince, R De Tayrac, and V Letouzey. Prevention and treatment of intra-uterine synechiae: review of the literature. *Journal de Gynecologie, Obstetrique et Biologie de la Reproduction,* 2014, 44(4): 366-379.

[3] C B Nagori, S Y Panchal, and H Patel. Endometrial regeneration using autologous adult stem cells followed by conception by in vitro fertilization in a patient of severe Asherman's syndrome. *Journal of Human Reproductive Sciences,* 2011, 4(1): 43.

[4] Y Zhang *et al.* Endometrial stem cells repair injured endometrium and induce angiogenesis via AKT and ERK pathways. *Reproduction (Cambridge, England),* 2016, 152(5): 389-402.

[5] J Tan *et al.* Autologous menstrual blood-derived stromal cells transplantation for severe Asherman's syndrome. *Human Reproduction,* 2016, 31(12): 2723-2729.

[6] J Burgner-Kahrs, D C Rucker, and H Choset. Continuum robots for medical applications: A survey. *IEEE Transactions on Robotics,* 2015, 31(6): 1261-1280.

[7] J Xiao, Y Yang, D Li, L Huang and L Zhang. Advances and Key Techniques of Ophthalmic Microsurgical Robots. *Journal of Mechanical Engineering,* 2013, 49(1): 1-8.

[8] K Xu, J Zhao, and M Fu. Development of the SJTU unfoldable robotic system (SURS) for single port laparoscopy. *IEEE/ASME Transactions on Mechatronics,* 2014, 20(5): 2133-2145.

[9] N Jang *et al.* Compact and Lightweight End-Effectors to Drive Hand-Operated Surgical Instruments for Robot-Assisted Microsurgery. *IEEE/ASME Transactions on Mechatronics,* 2020, 25(4): 1933-1943.

[10] L Luko, A Parush, and L Lowenstein. Cognitive task analysis of spatial skills in hysterectomy with the da Vinci surgical system. in *2017 13th IASTED International Conference on Biomedical Engineering (BioMed)*, 2017: 100-107.

[11] L Lowenstein, E Matanes, Z Weiner, and J Baekelandt. Robotic transvaginal natural orifice transluminal endoscopic surgery for bilateral salpingo oophorectomy. *European Journal of Obstetrics & Gynecology and Reproductive Biology.* 2020, 7: 100113.

[12] Y He, B Zhao, X Qi, S Li, Y Yang, and Y Hu. Automatic Surgical Field of View Control in Robot-Assisted Nasal Surgery. *IEEE Robotics and Automation Letters,* 2020, 6(1): 247-254.

[13] E Amanov *et al.* Transurethral Anastomosis after Transurethral Radical Prostatectomy: A Phantom Study on Intraluminal Suturing With Concentric Tube Robots. *IEEE Transactions on Medical Robotics and Bionics,* 2020, 2(4): 578-581.

[14] R E Goldman, A Bajo, L S MacLachlan, R Pickens, S D Herrell, and N Simaan. Design and performance evaluation of a minimally invasive telerobotic platform for transurethral surveillance and intervention. *IEEE Transactions on Biomedical Engineering,* 2012, 60(4): 918-925.

[15] A Bajo, L M Dharamsi, J L Netterville, C G Garrett, and N Simaan. Robotic-assisted micro-surgery of the throat: The trans-nasal approach. in *2013 IEEE International*

Conference on Robotics and Automation, 2013: 232-238.
[16] J Shang *et al.* A single-port robotic system for transanal microsurgery—Design and validation. *IEEE robotics and Automation Letters,* 2017, 2(3): 1510-1517,.
[17] K C Lau, E Y Y Leung, P W Y Chiu, Y Yam, J Y W Lau, and C C Y Poon. A flexible surgical robotic system for removal of early-stage gastrointestinal cancers by endoscopic submucosal dissection. *IEEE Transactions on Industrial Informatics,* 2016, 12(6): 2365-2374.
[18] C Freschi, V Ferrari, F Melfi, M Ferrari, F Mosca, and A Cuschieri. Technical review of the da Vinci surgical telemanipulator. *International Journal of Medical Robotics and Computer Assisted Surgery,* 2013, 9(4): 396-406.
[19] C He, L Huang, Y Yang, Q Liang, and Y Li. Research and realization of a master-slave robotic system for retinal vascular bypass surgery. *Chinese Journal of Mechanical Engineering,* 2018, 31(1): 1-10.
[20] C K Kim *et al.* Three-degrees-of-freedom passive gravity compensation mechanism applicable to robotic arm with remote center of motion for minimally invasive surgery. *IEEE Robotics and Automation Letters,* 2019, 4(4): 3473-3480.
[21] N Aghakhani, M Geravand, N Shahriari, M Vendittelli, and G Oriolo. Task control with remote center of motion constraint for minimally invasive robotic surgery. *IEEE international conference on robotics and automation*, 2013: 5807-5812.
[22] H Sadeghian, F Zokaei, and S Hadian Jazi. Constrained Kinematic Control in Minimally Invasive Robotic Surgery Subject to Remote Center of Motion Constraint. *Journal of Intelligent & Robotic Systems,* 2018, 95(3-4): 901-913.
[23] H Azimian, R V Patel, and M D Naish. On constrained manipulation in robotics-assisted minimally invasive surgery. *Biomedical Robotics and Biomechatronics (BioRob), 2010 3rd IEEE RAS and EMBS International Conference on*, 2010.
[24] J Sandoval, G Poisson, and P Vieyres. A New Kinematic Formulation of the RCM Constraint for Redundant Torque-Controlled Robots. *2017 Ieee/Rsj International Conference on Intelligent Robots and Systems (Iros),* 2017: 4576-4581.
[25] J Sandoval, G Poisson, and P Vieyres. Improved Dynamic Formulation for Decoupled Cartesian Admittance Control and RCM Constraint. *2016 Ieee International Conference on Robotics and Automation (Icra),* 2016: 1124-1129.
[26] H Su, S Li, J Manivannan, L Bascetta, G Ferrigno, and E De Momi. Manipulability Optimization Control of a Serial Redundant Robot for Robot-assisted Minimally Invasive Surgery. *2019 International Conference on Robotics and Automation (Icra),* 2019: 1323-1328.
[27] H Su, C Yang, G Ferrigno, and E De Momi. Improved Human–Robot Collaborative Control of Redundant Robot for Teleoperated Minimally Invasive Surgery. *IEEE Robotics and Automation Letters,* 2019, 4(2): 1447-1453.
[28] X Zhang, W Li, P W Y Chiu, and Z Li. A Novel Flexible Robotic Endoscope With Constrained Tendon-Driven Continuum Mechanism. *IEEE Robotics and Automation Letters,* 2020, 5(2): 1366-1372.
[29] J Li, Y Zhou, J Tan, Z Wang, and H Liu. Design and Modeling of a Parallel Shifted-Routing Cable-Driven Continuum Manipulator for Endometrial Regeneration Surgery. *2020 IEEE/RSJ International Conference on Intelligent Robots and Systems (IROS)*, 2020.
[30] J Li, Y Zhou, C Wang, Z Wang, and H Liu. A Model-Based Method for Predicting the Shapes of Planar Single-Segment Continuum Manipulators With Consideration of Friction and External Force. *Journal of Mechanisms and Robotics,* 2020, 12(4): 1-30.

Biographical notes

Jian-Hua Li, born in 1992, is currently a PhD candidate at *State Key Laboratory of Robotics, Shenyang Institute of Automation, Chinese Academy of Sciences, and University of Chinese Academy of Science, China*. He received his bachelor degree from *Central South University, China*, in 2016. His research interests include medical robots and systems, continuum robots, and robot control.
E-mail: lijianhua@sia.com

Chong-Yang Wang, born in 1991, is currently a research assistant at *Shenyang Institute of Automation, Chinese Academy of Sciences, China*. He received the B.E. and M.E. degrees from *Harbin Institute of Technology, China*, in 2013 and 2015, respectively. His research interests include surgical robots, medical sensors and robot control.
E-mail: wangchongyang@sia.cn.

Zhen-Xing Wang, born in 1995, is currently a PhD candidate at *State Key Laboratory of Robotics, Shenyang Institute of Automation, Chinese Academy of Sciences, and University of Chinese Academy of Science, China*. He received his bachelor degree from *Taiyuan University of Technology, China*, in 2018. His research interests include design and control of surgical robotics, continuum robots, and human–robot interaction.
E-mail: wangzhenxing@sia.com

Xiong Zheng, born in 1996, is currently a master degree candidate of *Mechanical Engineering College of Shenyang Jianzhu University, China*. He received his bachelor degree from *Anhui Jianzhu University, China*, in 2019. His research interests include medical robots and systems, vascular interventional surgery robots and robot control.
E-mail: zhengxiong312@163.com

Zhi-Dong Wang, is currently a Professor at the *Department of Advance Robotics, Chiba Institute of Technology, Japan*. He received the B.S. degree from the *Beijing University of Aeronautics and Astronautics, Beijing, China*, in 1987. He received the M.S. and Ph.D. degrees from the *Graduate School of Engineering, Tohoku University, Sendai, Japan*, in 1992 and 1995, respectively. His current research interests include human-robot interaction and cooperation systems, distributed autonomous robot systems, micro/nano robotics, and application of intelligent robot technologies for the disabled
E-mail: Zhidong.wang@it-chiba.ac.jp

Ji-Chun Tan, born in 1965, is a professor at *Shengjing Hospital Affiliated to China Medical University, China*. She received the B.S., M.S. and Ph.D. degrees from *Jilin University, China,* in 1986, 1989 and 2003, respectively. Her research interests include

infertility, assisted reproductive technology, stem cells, and surgical robot.
E-mail: tjczjh@163.com

Hao Liu, born in 1980, is currently a professor at *Shenyang Institute of Automation, Chinese Academy of Sciences, China*. He received the B.S., M.S., and Ph.D. degrees from the *Harbin Institute of Technology, China*, in 2004, 2006, and 2010, respectively. He worked as a visiting scholar in *Laboratory for Computational Sensing and Robotics, Johns Hopkins University, United States of America* from 2014-2015. His research interests include surgical robots, medical sensors, surgical navigation, and robot control.
Tel: +86-024- 83602067; E-mail: liuhao@sia.cn

Supplementary Files

This is a list of supplementary files associated with this preprint. Click to download.

- MasterslavecontrolwithRCMconstraint.wmv